BMC Genomics

RESEARCH

Open Access

Gene ontology defines pre-post- hatch energy dynamics in the complexus muscle of broiler chickens

Jonathan Dayan[1] and Zehava Uni[1*]

Abstract

Background Chicken embryos emerge from their shell by the piercing movement of the hatching muscle. Although considered a key player during hatching, with activity that imposes a substantial metabolic demand, data are still limited. The study provides a bioenergetic and transcriptomic analyses during the pre-post-hatching period.

Methods Weight and morphology alongside content determination of creatine and glycogen were analysed. Transcriptome identified differentially expressed genes and enriched biological processes associated with hatching muscle development, catabolism, and energy provision. Using gene set enrichment, we followed the dynamics of gene-sets involved in energy pathways of oxidative phosphorylation, protein catabolism, glycolysis/gluconeogenesis, and glycogen metabolism.

Results Results show several significant findings: (A) Creatine plays a crucial role in the energy metabolism of the hatching muscle, with its concentration remaining stable while glycogen concentration is depleted at hatch and placement. (B) The hatching muscle has the capacity for de-novo creatine synthesis, as indicated by the expression of related genes (AGAT, GAMT). (C) Transcriptome provided insights into genes related to energy pathways under conditions of pre-hatch oxygen and post-hatch glucose limitations (oxidative phosphorylation: NDUF, MT-ND, SDH, UQCR, COX, MT-CO, ATP5, MT-ATP; glycolysis/gluconeogenesis: FBP,G6PC, PFKM; glycogen metabolism: PPP1, PYGL, GYG1). (D) The post-hatch upregulation of protein catabolic processes genes (PSMA, RNF, UBE, FBX), which align with the muscle's weight dynamics, indicates a functional shift from movement during hatching to lifting the head during feeding.

Conclusions There is a dynamic metabolic switch in the hatching muscle during embryo-to-hatchling transition. When glycogen concentration depletes, energy supply is maintained by creatine and its de-novo synthesis. Understanding the hatching muscle's energy dynamics is crucial, for reducing hatching failures in endangered avian species, and in domesticated chickens.

Keywords Hatching Muscle, Pipping Muscle, Embryo, Hatching chick, Mars-seq, Creatine, Glycogen, Histology

Background

Birds rely on successful emergence from their shell to complete their embryonic development [1, 2]. The hatching muscle (complexus muscle), located in the upper cervical region, is responsible for the piercing movement necessary to exit the calcified shell [3]. It employs independent nerve control to coordinate vigorous muscle activity and movements [4]. The hatching

*Correspondence:
Zehava Uni
Zehava.uni@mail.huji.ac.il
[1] Department of Animal Science, The Robert H. Smith Faculty of Agriculture, Food, and Environment, The Hebrew University of Jerusalem, 7610001 Rehovot, Israel

muscle consists primarily of glycolytic muscle fibers, functioning during hatching, while a minority is oxidative-glycolytic fibers, which start functioning after hatch [5].

All muscle activities require the breakdown of adenosine triphosphate (ATP) and the release of free energy [6]. However, as only a relatively small amount of ATP is stored within the body's cells [7], ATP turnover relies on energy storage molecules such as glycogen and triacylglycerols and also ATP regeneration by three primary energy systems: mitochondrial respiration, the glycolytic system, and the phosphagen (creatine/phosphocreatine) system [8]. These systems differ by the amount of generated ATP and turnover rate. Mitochondrial respiration, the most sizable ATP supply system, generates approximately 30–32 ATP molecules at a relatively slow turnover rate. In contrast, glycolysis yields only 2 ATP molecules but with a higher turnover rate, and the phosphagen system, being the fastest way of ATP provision, yields only 1 ATP per cycle [8, 9]. Thus, a view on these energy systems reflects on the muscle bioenergetic status.

The hatching muscle, as a key player during hatching, imposes a substantial metabolic demand [2, 5, 10]. Advancing our understanding of its energy metabolism may provide insights to reduce hatching failures, a matter of scientific and economic importance. A multilevel meta-analysis estimated hatching failures in birds to affect around 16.79% of all eggs laid [11], with domesticated birds experiencing a rate of about 10%, while some endangered populations face hatching failure rates of up to 75% [12]. As meat-type (broiler) chickens' domestication is considered relatively recent [13, 14] and as the hatching muscle shares characteristics with other birds such as North American Grebes [15], it is plausible that bioenergetic processes are also conserved across species. Thus, our animal model is instrumental not only in meeting the ever-growing demand for day-old chicks, a crucial component of the broiler industry [16], but also in conservation efforts for endangered species. Despite all that, data about the metabolic and molecular processes in the hatching muscle are still limited.

A large body of evidence comes from studies performed on the chick. During the embryo-to-hatchling transition period, the hatching muscle experiences dramatic morphological changes. Starting on embryonic day (E) 17 and until hatching on E21, this muscle undergoes rapid 'lymph-like' infiltration of fluids and glycogen granules [17, 18]. The extensive infiltration eventually separates individual muscle bundles and fibers while maintaining their functional contraction capability [19]. Post-hatch, the muscle's size decreases as the 'lymph-like' function declines. Then, the muscle undergoes a transition, taking on its new role as the complexus muscle, which acts in lifting the head during feeding [4, 20].

This study provides a bioenergetic and transcriptomic view of the hatching muscle in domesticated broiler chickens, from the late-embryonic stage (last week of incubation) until hatch and chick placement. We investigated weight and morphological changes in the hatching muscle alongside content determination of two high-energy value molecules: creatine and glycogen. Additionally, transcriptomic analysis identified differentially expressed genes and enriched biological processes associated with hatching muscle development, catabolism, and energy provision. Using gene set enrichment analysis, we followed the dynamics of specific gene sets involved in energy provision pathways of oxidative phosphorylation, protein catabolism, glycolysis/gluconeogenesis, and glycogen metabolism.

Results

Hatching muscle weight and morphology

Measurements of hatching muscle weight (E15- 0.18 g, E17- 0.30 g, E19- 0.79 g, hatch-0.87 g, placement-0.52 g) revealed a significant increase during the last week of incubation (Fig. 1G). A remarkable 4.8-fold change between embryonic day (E)15 and hatch ($P<0.0001$). This weight increase correspond with images showing a macroscopic view of the hatching muscle on E17, E19, and at hatch (Fig. 1A-C), and a microscopic view by H&E-stained images (Fig. 1D-F). These images also indicate the separation between muscle bundles and myofibers which may be the result of 'lymph-like' infiltration (Fig. 1D-F). A notable decrease in tissue weight was observed with a 67% reduction during the 24 h from the moment of hatch until chick placement at the farm ($P<0.0001$).

Creatine and glycogen content determination

The glycogen concentration (mg/g dry weight) in the hatching muscle exhibited dramatic fluctuations up to hatch, observed at 48-h intervals (Fig. 2A). Levels increased by 1.6-fold between E15 to E17 ($P=0.0005$) and then sharply decreased by twofold between E19 and hatch ($P<0.0001$). At chick placement, glycogen concertation was lowest (6.13 ± 1.65), fivefold lower compared to the highest level at E17 (32.14 ± 2.49, $P<0.0001$). Similar dynamics were observed in total glycogen amount (mg), calculated by multiplying the total tissue weight by the glycogen concentration (Fig. 2B). The total amount of hatching muscle glycogen was the highest at E19. Yet no significant differences were observed in either amount or concentration between E17 and E19. Creatine concentration (mg/g dry weight) and total amount (mg) remained constant between E17 and chick placement. In just 48 h between E15 and E17, a 1.5-fold increase in creatine

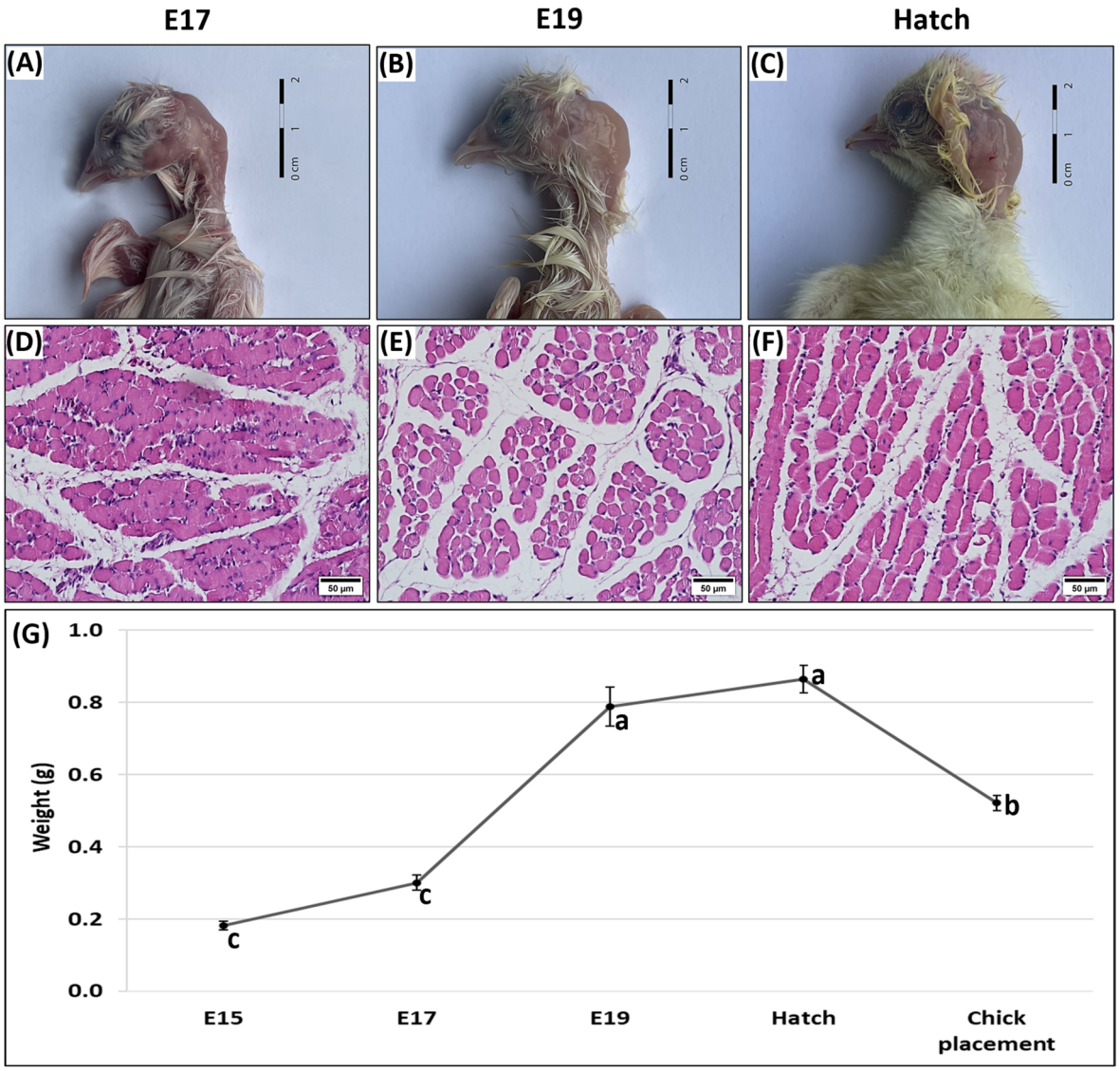

Fig. 1 A view of the hatching muscle during the last week of chicken embryonic development. **A**-**C** Images showing a macroscopic view of the hatching muscle on E17, E19 and at hatch. **D**-**F** Histological images showing microscopic view (X40 magnification) were stained with H&E and generated using EVOS FL Auto-inverted microscope on E17, E19 and at hatch. 'Lymph like' accumulation and increased myofiber size are evident between E17 to E19 and hatch. **G** Weight data on embryonic day (**E**) 15, E17, E19, at hatch and at chick placement. Lowercase letters denote for means that are significantly different between days, as derived from one-way ANOVA followed by Tukey's HSD test ($p \leq 0.05$), $n = 6$ birds/day

concentration was observed (Fig. 2A, $P = 0.002$) and also a 2.9-fold increase in creatine total amount (Fig. 2B, $P < 0.0001$).

A comparison between the two energy supply molecules (i.e., glycogen and creatine) within each examined day shows that on E15, E17, and E19, glycogen levels were significantly higher compared to creatine ($P < 0.005$). For example, the amount of glycogen (mg) in E19 was 2.71 ± 0.22, while the amount of creatine (mg) was 1.12 ± 0.04 (Fig. 2B). At hatch, both molecules had the exact amounts in the hatching muscle. At placement, although both creatine and glycogen amounts showed a significant decrease, creatine levels (1.08 ± 0.07) were doubled compared to glycogen (0.51 ± 0.16, $P < 0.01$).

Gene clustering and ontology

A transcriptomic clustering analysis was performed to track time-course expression patterns in the hatching muscle of chickens during the embryo-to-hatchling transition period. A total of 917 differentially expressed (DE) genes across 5 clusters were identified based on $P < 0.05$ after false discovery rate (FDR) correction. Figure 3A

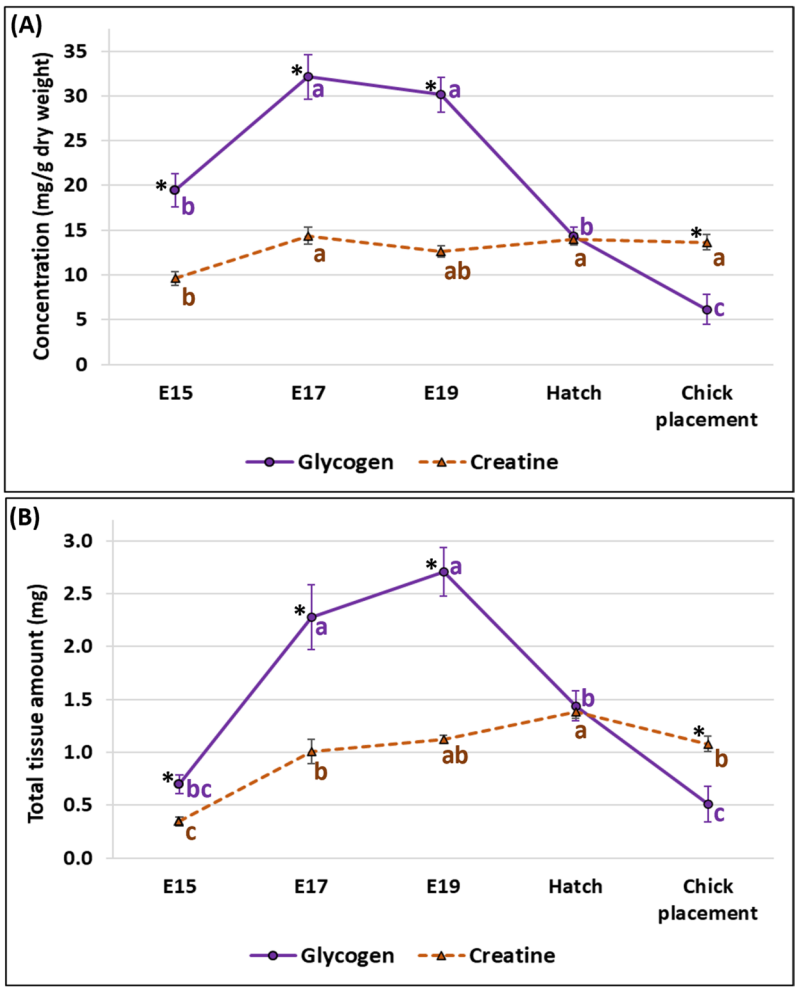

Fig. 2 Levels of creatine and glycogen in the hatching muscle on embryonic day (**E**) 15, E17, E19, at hatch and at chick placement at the farm. **A** The concentration of creatine and glycogen (mg/g dry weight tissue) were determined, and (**B**) the total amount (mg) was calculated to demonstrate the full capacity of energy storage in tissue. Asterisks denote for means that are significantly different between the levels of creatine and glycogen for each day, as derived from one-way ANOVA followed by Student's t-test ($p \leq 0.05$). Lowercase letters denote for means that are significantly different between days for the levels each energy molecule (creatine and glycogen), as derived from one-way ANOVA followed by Tukey's HSD test ($p \leq 0.05$). $n = 6$ birds/day

presents the cluster heatmap of DE genes across examined days, with comparisons as follows: E17 vs. E15, E19 vs. E17, Hatch vs. E19, and Placement vs. Hatch.

Cluster 1 included 201 DE genes (Fig. 3A). Their expression pattern indicated the highest expression at E15, then gradually decreasing along E17, E19, hatch, and placement. The gene ontology of biological processes (GOBP) revealed a significant enrichment of the creatine metabolic process related to the energy provision pathways (Fig. 3B). Among enriched genes are L-arginine amidinotransferase (AGAT) and guanidinoacetate N-methyltransferase (GAMT), which is responsible for the de novo synthesis of creatine. Other processes were mainly related to muscle support system development, including collagen fibril organization, extracellular organization, muscle structure, tendon, and circulatory system development.

Cluster 2 included 172 DE genes showcasing a dynamic expression pattern, gradually increasing between E15 to E19 and rapidly decreasing at hatch and chick placement (Fig. 3A). The GOBP enrichment (Fig. 3C) revealed processes pivotal for energy provision: glycolysis/gluconeogenesis and glucose metabolism. In addition, significant enrichments were observed in processes associated with the build-up of the hatching muscle. These include skeletal and cardiac muscle tissue development, cell differentiation, sarcomere organization, muscle contraction, and actin-myosin filament sliding.

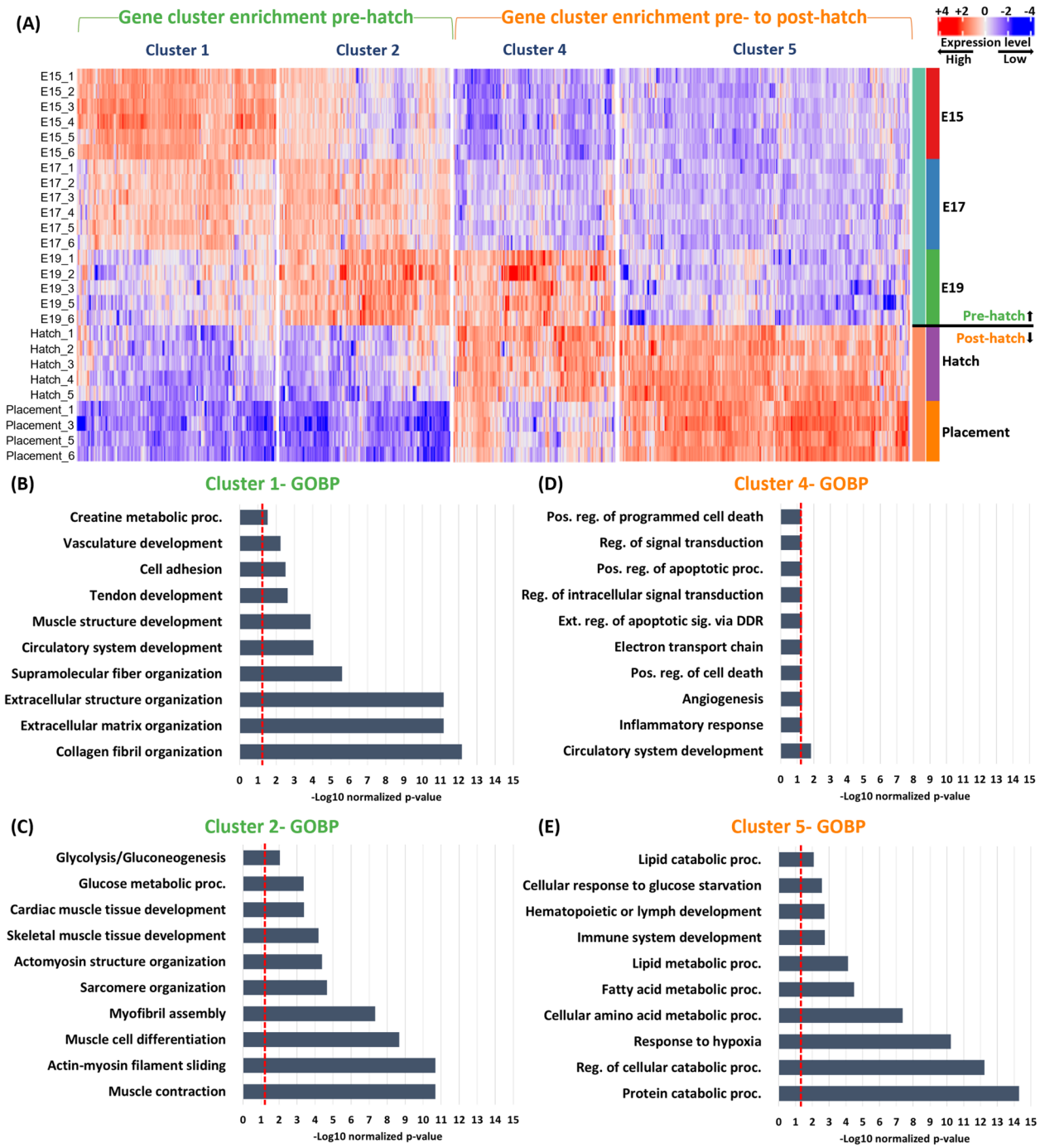

Fig. 3 Gene clustering enrichment outputs and gene ontology of biological processes (GOBP). **A** Presents gene clustering heatmap, evaluation along days (E15-E17-E19-Hatch-Placement) and before vs. after hatching. **B**-**C** GOBP by cluster, showing direct terms that were significantly enriched indicating activation before (**B**) or after (**C**) hatching. Data is presented as '-Log10 normalized *p*-value' representing the level of significance based on false discovery rate (FDR) *p*-value correction. The red dash line represents the significance threshold at $P < 0.05$ level. Bars exceeding the threshold were significantly enriched, no significant enrichments were found in cluster 3

Cluster 3 included 87 genes. No significant enrichment representative of a specific biological process or function was found within this cluster (Supplementary Fig. 1).

Cluster 4 included 163 DE genes (Fig. 3A). Their expression was almost completely shut down at E15 and E17. At E19, expression dramatically peaked, maintaining

a high level at hatch, followed by a decrease at placement. GOBP enrichments (Fig. 3D) were just at the significant threshold and involved processes mainly related to signal transduction and programmed cell death. Additionally, gene enrichments associated with circulatory system development, inflammatory response, and energy provision via the mitochondrial electron transport chain were identified.

Cluster 5 included 294 DE genes and exhibited a dichotomous expression pattern between pre- and post-hatching days (Fig. 3A). On pre-hatch days (E15, E17, E19), expression levels of genes in this cluster were suppressed, while on post-hatch days (hatch, placement), expression levels of these genes were boosted. GOBP enrichments in this cluster (Fig. 3E) involved lipid and protein catabolic processes, and lipid, fatty acid, and amino acid metabolic processes. In addition, processes related to immune system development, hematopoietic/lymph development, and response to hypoxia and glucose starvation.

Gene set enrichment analysis

Different from a clustering analysis, which initially identifies DE genes and later links them to specific biological processes, a gene set enrichment analysis (GSEA) utilizes pre-defined sets of genes to determine significant differences (based on $P<0.05$ after FDR correction) in specific biological processes between two biological states. This approach enabled us to analyze 7083 identified genes linked to 2639 gene sets. We focused on four biological processes related to energy provision pathways in the hatching muscle: oxidative phosphorylation, protein catabolic process, glycolysis/gluconeogenesis, and glycogen metabolism. Figure 4 compares consecutive days (E17 vs. E15; E19 vs. E17; Hatch vs. E19; Placement vs. Hatch) when a positive parabola indicates that most gene set members were upregulated. In contrast, a negative parabola indicates that most gene set members were distributed in a downregulated manner.

The GSEA identified 92 genes related to oxidative phosphorylation, indicating the mitochondrial electron transport chain (Fig. 4; GSEA supplementary data). Among them are genes of mitochondrial complex 1 [NADH: ubiquinone oxidoreductase subunits (NDUF, MT-ND)], mitochondrial complex 2 [succinate dehydrogenase subunits (SDH)], mitochondrial complex 3 [ubiquinol-cytochrome c reductase complex subunits (UQCR)], mitochondrial complex 4 [cytochrome c oxidase subunits (COX, MT-CO)], and mitochondrial complex 5 [ATP synthase subunits (ATP5, MT-ATP)]. The oxidative phosphorylation gene set expression profile indicated upregulation when comparing E17 to E15 (85% of the genes were upregulated), upregulation on E19 compared to E17 (64% of the genes were upregulated), and downregulation when comparing between hatch and E19 (61% of the genes were downregulated). No significant gene set enrichments were found between placement and hatch.

Analysis of the protein catabolic process identified 545 related genes (Fig. 4; GSEA supplementary data). The four largest gene groups, representing almost 20%

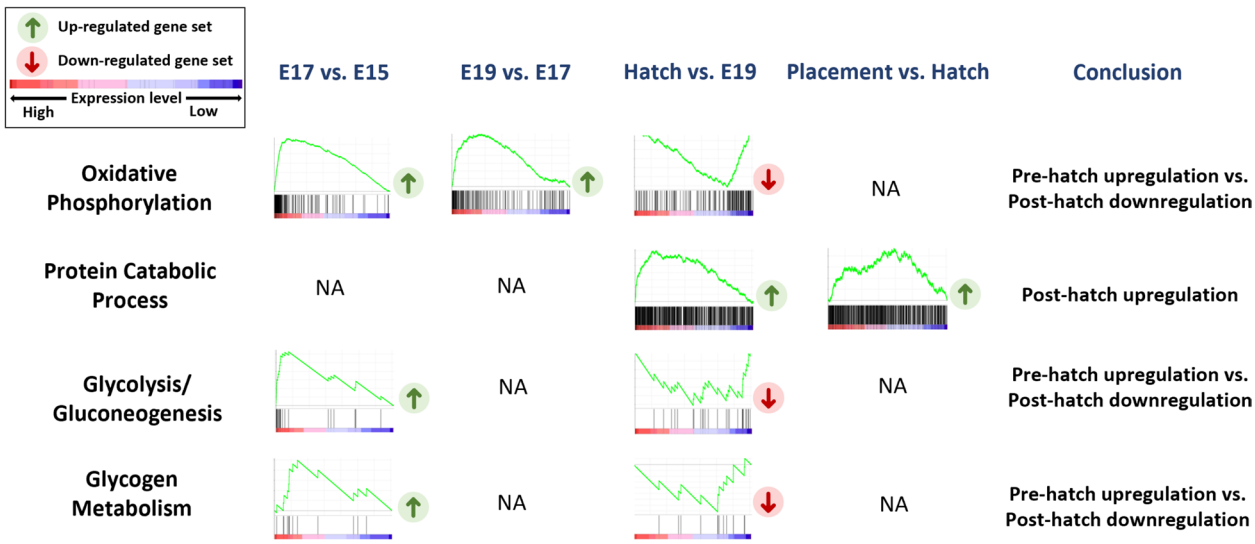

Fig. 4 Gene set enrichment analysis (GSEA) of biological processes (BP) related to energy provision pathways (Oxidative Phosphorylation; Protein Catabolic Process; Glycolysis/Gluconeogenesis; Glycogen Metabolism). Comparisons between days (E17-E15; E19_E17; Hatch_E19; Placement_Hatch) of gene sets that are enriched in up or down-regulated manner and Not Applicable (NA, gene set is not enriched). FDR False discovery rate (FDR) *p*-value correction of $P<0.05$, represents the significance threshold

of identified genes, are proteasome alpha (PSMA) subunits, RING finger (RNF) proteins, Ubiquitin-protein ligase E (UBE) subunits, and the F-box (FBX) gene family. Significant protein catabolic process gene set enrichments were observed between hatch and E19 and between placement and hatch, with 51% and 64% upregulation, respectively.

Glycolysis/Gluconeogenesis GSEA revealed 26 genes (Fig. 4; GSEA supplementary data). Among them are three genes encoding key rate-limiting enzymes: fructose-1,6-bisphosphatase (FBP), Phosphofructokinase muscle (PFKM), and glucose-6-phosphatase (G6PC). Significant gene set enrichment was found on E17 compared to E15 when 73% of the analysed genes were upregulated. Opposingly, when comparing between hatch and E19, 81% of the analysed genes were downregulated. No significant enrichments were found between E19 to E17 and between placement to hatch.

Interestingly, a similar expression profile was observed in the analysis of 13 genes related to glycogen metabolism (Fig. 4; GSEA supplementary data). Compared to E15, 69% of analysed genes were upregulated on E17, while between hatch to E19, 69% of genes were downregulated. These genes include the glycogen phosphorylase L (PYGL), glycogenin-1 (GYG1), and phosphoprotein phosphatase 1 (PPP1) gene family.

Together, GSEA indicted pre-hatch upregulation vs. post-hatch downregulation in gene sets involved in energy provision pathways of oxidative phosphorylation, glycolysis/gluconeogenesis, and glycogen metabolism and post-hatch upregulation in gene sets involved in protein catabolism.

Discussion

This study provides new insights on energy dynamics in the broiler chick hatching muscle during the pre-post-hatching period through measurements of weight and morphology, creatine and glycogen content determination, and transcriptomic analysis (Fig. 5). The study aims to better understand the metabolism of the hatching muscle energy that supports its activity and enables the embryo to pierce its way out of the shell.

The nearly fivefold increase in hatching muscle weight from E15 to hatch, together with our macroscopic and histological observations, is plausibly the result of the rapid 'lymph-like' infiltration of fluids and glycogen granules. These results agree with previous studies that portray the muscle -weight dynamics and energy-storing capacity required to support the intense muscle activity during hatching [17, 18]. The observed separation between muscle bundles and myofibers (as shown in the H&E images in Fig. 1) may result from extensive 'lymph-like' infiltration, as suggested in previous research [19]. The rapid decrease in muscle weight within 24 h from the moment of hatching at placement is suggested to be related to functional adaptation in the muscle from facilitating hatching to enabling feeding [4, 20].

To meet the high metabolic demands during hatching, a rapid utilization of glycogen take place [5]. This was portrayed by the dramatic decrease in glycogen concentration and amount in the hatching muscle towards hatch. A similar pattern was demonstrated in the embryonic liver, breast muscle, and the extraembryonic yolk sac (YS) tissue corresponding with the changes in energy metabolism and increased energy demands [21–28]. Remarkably, when hatching muscle glycogen concentration depleted, creatine concentration remained sustained, highlighting its importance to embryos and

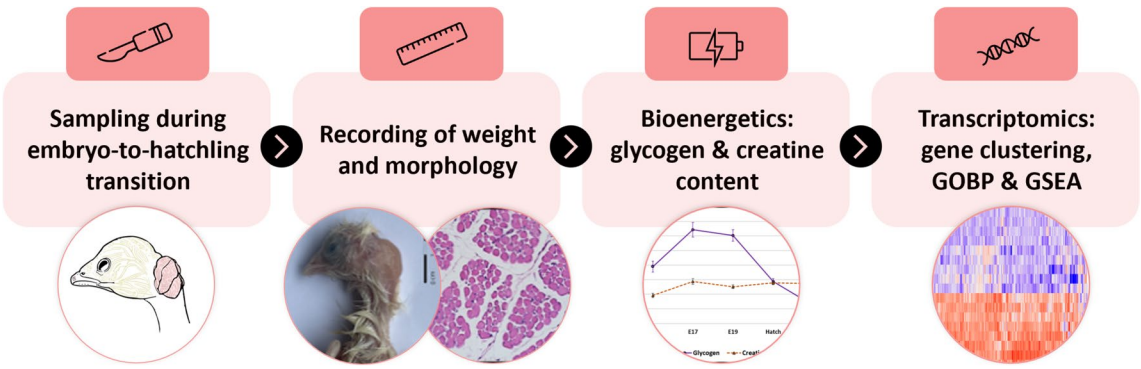

Fig. 5 Experimental design. The study investigates bioenergetic and transcriptomic profiles in the hatching muscle of chickens from late-embryonic development until hatch and chick placement. We recorded weight and morphological changes alongside assessments of creatine and glycogen stores, combining histological analysis and content evaluation. Transcriptomic analysis included gene clustering enrichment outputs, gene ontology of biological processes (GOBP), and gene set enrichment analysis (GSEA), all associated with hatching muscle development, catabolism, and energy provision pathways

hatchlings. This phenomenon was also demonstrated in the breast muscle [28].

Transcriptomic clustering, conducted for the first time in the chick hatching muscle, indicated dynamic changes in energy pathways related to the physiological limitations in oxygen and glucose levels in the pre-hatch and post-hatch periods, respectively. Cluster 1, with 201 DE genes, showed the highest expression levels at E15, which decreased over time. The GOBP revealed a significant enrichment in creatine metabolism. This includes genes encoding for the two enzymes responsible for the de-novo synthesis of creatine: L-arginine: glycine amidinotransferase (AGAT), catalyzing the reaction between glycine and arginine to create ornithine and guanidinoacetic acid and guanidinoacetate N-methyltransferase (GAMT), responsible for GAA methylation via S-adenosylmethionine to form creatine [9, 29]. This study is the first to demonstrate the hatching muscle's potential to synthesize creatine, a capability previously shown in the skeletal muscles of fish, mice, cattle, and pigs [30] and in the breast muscle of chickens [28]. The ability of the hatching muscle to synthesize its own creatine may explain the sustained creatine levels post-hatch, facilitating a metabolic advantage by maintaining muscle creatine levels and cellular energy [31]. Cluster 2 included 172 DE genes, linked to energy pathways of glycolysis, gluconeogenesis, and glucose metabolism; their expression levels increased until E19. During hatching, the muscle activity strongly relies on glycolysis from glucose provided by the glycogen reserves [32]. Once glycogen levels were depleted at hatch and placement, expression dynamics indicated a downregulation of glycolysis, gluconeogenesis, and glucose metabolism pathways. Similar patterns of expression were observed in the liver, YS tissue, and breast muscle, where their dynamics changed according to oxygen and glucose availability [2, 5, 26–28, 33]. GOBP of clusters 1 and 2 also included processes associated with the build-up of the hatching muscle and its support system development. The expression pattern corresponds with our results and results from previous studies, showing the growth dynamics of the hatching muscle [17, 18, 34]. Clusters 4 and 5 showed similar patterns. Cluster 4 contained 163 DE genes with expression shut down at E15 and E17, and then peaking at E19 onwards. Cluster 5, with 294 DE genes, exhibited suppressed pre-hatch and boosted post-hatch expression. GOBP of cluster 4 included mitochondrial electron transport chain genes, and GOBP enrichments in cluster 5 involved lipid, fatty acid, and amino acid metabolic processes, as well as processes related to immune system development, hematopoietic/lymph development, and response to hypoxia and glucose starvation. Their enrichment towards and post-hatch periods may be linked to the oxygen status and the high energy demand of the hatching process [2, 5, 33, 35]. Once the beak pierces the shell, pulmonary functioning provides adequate O_2 for fatty acid catabolism to resume as a source of energy [36, 37]. This is indicated in the GOBP of clusters 4 and 5 with genes related to lipid and protein catabolism, signal transduction, and programmed cell death. The biological processes of clusters 4 and 5 are probably also linked to the observed weight decrease post-hatch, as the muscle undergoes a transition from shell piercing movement to movement during feeding [4, 20].

The gene set enrichment analysis (GSEA) focused on four biological processes: oxidative phosphorylation, protein catabolic process, glycolysis/gluconeogenesis, and glycogen metabolism. The comparison matrix examined differences between consecutive days (E17 vs. E15; E19 vs. E17; Hatch vs. E19; Placement vs. Hatch). The GSEA for oxidative phosphorylation identified 92 related genes, indicating energy provision by the mitochondrial electron transport chain. The observed upregulation towards E19 shows a similar pattern to cluster 4, with an expression peak on E19. The detailed view of GSEA shows that from E15 to E19, the mitochondrial electron transport chain functions effectively, as indicated by the upregulation of the oxidative phosphorylation process. The downregulation observed between E19, hatch, and placement may be related to the muscle's response to oxygen and glucose starvation, as indicated in the GOBP of cluster 5 and by the sharp decrease in glycogen levels towards hatch. Glucose deficiency has been shown to induce oxidative stress and mitochondrial dysfunction [38–40]. GSEA of the protein catabolic process identified 545 related genes. The observed enrichments post-hatch perfectly align with the expression boost presented in cluster 5, indicating muscle tissue degradation and a functional shift. GSEA of Glycolysis/Gluconeogenesis (26 genes) and glycogen metabolism (13 genes) indicate that the high expression levels between E17 and E15 were maintained until E19, and then, between E19 and hatch, downregulation was observed. These results are in similarity to the process indicated in cluster 2. As seen previously in the liver, YS tissue, and breast muscle [28], the decreased activity of these metabolic pathways fit the observed decrease in glycogen levels, suggesting poor energetic status in hatchlings.

Conclusion

This study has yielded notable findings. First, creatine's role in sustaining energy levels as glycogen reserves in the hatching muscle deplete highlights its importance. Second, de-novo synthesis of creatine is supported by active gene expression. Third, transcriptomic analysis reveals adaptive energy pathways to address pre-hatch

oxygen and post-hatch glucose limitations. Lastly, post-hatch upregulation of protein catabolism aligns with a functional shift, marking the muscle's transition from hatching activity to feeding adaptations, illustrating its dynamic developmental role during the embryo-to-hatchling transition. Given the hatching muscle's critical role and substantial metabolic demand during shell piercing, understanding its energy dynamics can provide valuable insights for reducing hatching failures, supporting conservation efforts for endangered species, and meeting the needs of the domesticated chicken industry. From an evolutionary perspective, the relative recentness of the chicken's domestication from its wild ancestor the red jungle fowl, and the similar hatching muscle characteristics found in other avian species, suggest that the generality of the aforementioned bioenergetic processes will be conserved, promising relevance to all avian species.

Methods

Eggs, incubation and sampling procedure

Fertile eggs ($n=100$; mean weight = 70.04 g, SD = 2.19 g) from 40-week-old broiler hens (Cobb 500) were purchased from a commercial breeder farm (Y. Brown and Sons Ltd., Hod Hasharon, Israel). Eggs were incubated in a Petersime hatchery at the Faculty of Agriculture of the Hebrew University under standard conditions (37.8 °C and 56% relative humidity). On embryonic day (E)10, eggs were candled, unfertilized eggs and dead embryo eggs were removed. Tissue sampling was performed at E15, E17, E19, at hatch (actual time of hatch at the hatchery) and at chick placement (24 h post hatch, prior to first feed at the farm). Sampling was conducted on randomly selected males, which were euthanized via cervical dislocation. Hatching muscle was removed, weighted and immediately was placed in liquid nitrogen and kept under −80°c until further processing. Muscles were analyzed for the following: (1) creatine and glycogen content determination (E15, E17, E19, hatch and chick placement, $n=6$ per day); (3) MARS-Seq transcriptome analysis (E15, E17, E19, hatch and chick placement, $n=6,6,5,5,4$ per day, respectively). For histology (E17, E19 and hatch, $n=4$ per day), muscles were immediately fixed in formaldehyde as described below. A summary of the experimental design appears in Fig. 5. The study was reviewed and approved by the Hebrew University Institutional Animal Care and Use Committee (IACUC): AG-20–16298.

Creatine and glycogen content determination

Frozen muscle samples were lyophilized and later examined for their creatine and glycogen content by Swiss-BioQuant-AG (Reinach, Switzerland). The concentration of creatine and glycogen (mg/g dry weight tissue) was determined, and the total tissue weight (mg) was calculated.

Histology

Muscle samples were obtained by removing the entire left half of the hatching muscle and were subsequently fixed in 3.7% formaldehyde in PBS at pH 7.4 (Sigma-Aldrich, Rehovot, Israel) for 24 h. Then, samples were dehydrated, cleared, and embedded in paraffin. Cross sections of 4–6 μm thick were cut, deparaffinized in Histochoice clearing agent (Sigma-Aldrich St. Louis, MO), rehydrated, and stained. After drying, samples were mounted on cover glass using DPX slide mounting medium (Sigma-Aldrich St. Louis, MO). Finally, images were captured using an EVOS FL Auto-inverted microscope with X40 magnification and analysed using Fiji ImageJ software (version 1.53t). Hematoxylin & Eosin (H&E) staining was used to allow a histological view of the hatching muscle tissue.

MARS-Seq and bioinformatics

Total RNA was isolated from 100 mg of frozen muscle tissue using TRI-Reagent (Sigma-Aldrich, St. Louis, MO) according to the manufacturer's protocol. RNA concentrations were determined using a Nano Drop ND-1000 instrument (Thermo Fisher Scientific, Wilmington, DE), and the integrity was assessed by Tape-Station (Agilent Technologies, Santa Clara, CA, USA). Of the initial 30 samples, 26 were ultimately analyzed, with NanoDrop ratios around ~ 2.0 and RNA Integrity Numbers (RIN) ranging between 8.1 and 9.8, ensuring high-quality data for further analysis. Sequencing Libraries were prepared using LIB_PREP_PROTOCOL. READ_TYPE, 75 bp single reads were sequenced on NUM_LANES lane(s) of an Illumina ILLUMINA_INSTRUMENT. The output was ~ 16 million reads per sample [The Nancy and Stephen Grand Israel National Center for Personalized Medicine. The Weizmann Institute of Science, Rehovot, Israel (http://g-incpm.weizmann.ac.il/)]. Poly-A/T stretches and Illumina adapters were trimmed from the reads using cut-adapt [41], resulting reads shorter than 30 bp were discarded. Remaining reads were mapped onto 3' UTR regions (1000 bases) of the Gallus, galGal7 genome according to Refseq annotations, using STAR 2.7.10a [42] with End-to-end option and out Filter Mismatch Nover Lmax was set to 0.05. Deduplication was carried out by flagging all reads that were mapped to the same gene and had the same UMI. Counts for each gene were quantified using HTSeq-count 2.0.2 [43], using the gene transfer format (GTF) above. UMI counts were corrected for saturation by considering the expected number of unique elements when sampling without replacement. Differentially expressed genes were identified using DESeq2 [44]

with the beta Prior, cooks Cutoff and independent Filtering parameters set to False. Raw *P* values were adjusted for multiple testing using the procedure of Benjamini and Hochberg. Pipeline was run using snake-make [45].

For bioinformatics advanced analysis, two approaches were applied to the expression data for identifying altered gene sets and pathways in the various biological states. In the first approach, genes from the various clusters were submitted for enrichment analysis using ShinyGO 0.76 [46], human orthologs were used, with the default parameters and background. In the second, whole expression data were submitted for gene set enrichment analysis (GSEA). GSEA was used to determine whether a priori defined sets of genes show statistically significant, concordant differences between two biological states [47]. The ortholog human genes were used for the analysis. The following gene sets databases were used: the hallmark collection from the molecular signatures database (MSigDB v2023.2.Hs), and gene ontology of biological process (GOBP).

Statistical analysis

Data of hatching muscle weight were subjected to one-way ANOVA, differences between days were tested by Tukey's HSD test. Data of creatine and glycogen content determination were subjected to one-way ANOVA, differences within each day were tested by Student' t-test and differences between days for each molecule were tested by Tukey's HSD test. Values are presented as mean ± standard error mean (SEM) and were considered significantly different with *P*-value lower than or equal to 0.05 ($P \leq 0.05$). All aforementioned analyses were carried out using JMP-pro 16 software (SAS Institute Inc., Cary, NC).

Abbreviations

ATP	Adenosine triphosphate
YS tissue	Yolk sac tissue
H&E	Hematoxylin & Eosin
GSEA	Gene set enrichment analysis
GOBP	Gene ontology of biological process
DE	Differentially expressed
FDR	False discovery rate
AGAT	L-arginine amidinotransferase
GAMT	Guanidinoacetate N-methyltransferase
NDUF, MT-ND	NADH: ubiquinone oxidoreductase subunits
SDH	Succinate dehydrogenase subunits
UQCR	Ubiquinol-cytochrome c reductase complex subunits
COX, MT-CO	Cytochrome c oxidase subunits
ATP5, MT-ATP	ATP synthase subunits
PSMA	Proteasome alpha subunits
RNF	RING finger proteins
UBE	Ubiquitin-protein ligase E subunits
FBX	F-box gene family
FBP	Fructose-1,6-bisphosphatase
PFKM	Phosphofructokinase muscle
G6PC	Glucose-6-phosphatase
PYGL	Glycogen phosphorylase L
GYG1	Glycogenin-1
PPP1	Phosphoprotein phosphatase 1 gene family

Supplementary Information

The online version contains supplementary material available at https://doi.org/10.1186/s12864-024-11103-6.

Supplementary Material 1.

Acknowledgements

A special thank you is extended to Prof. Orna Halevy, and Dr. Hadar Benyamini. Prof. Orna Halevy is acknowledged for her contribution to the review of this manuscript. Dr. Hadar Benyamini, from the I-CORE bioinformatics unit of the Hebrew University of Jerusalem, is acknowledged for advanced bioinformatic data analysis.

Authors' contributions

J.D. and Z.U. designed and executed the study, analyzed the data, and wrote the manuscript.

Funding

Not applicable.

Data availability

All data supporting the findings of this study are included in the paper, Supplementary Fig. 1, and the Mars-seq data, which are available in the Gene Expression Omnibus (GEO) repository (Accession: GSE282902; https://www.ncbi.nlm.nih.gov/geo/query/acc.cgi?acc=GSE282902). For further inquiries, please contact the corresponding author.
All data supporting the findings of this study are included in the paper, Supplementary

Declarations

Ethics approval and consent to participate

The study was reviewed and approved by the Hebrew University Institutional Animal Care and Use Committee (IACUC): AG-20–16298.

Consent for publication

Not applicable.

Competing interests

The authors declare no competing interests.

Received: 7 July 2024 Accepted: 28 November 2024
Published online: 04 December 2024

References

1. Pohlman AG. Concerning the causal factor in the hatching of the chick, with particular reference to the musculus complexus. Anat Rec. 1919;17:88–104. https://doi.org/10.1002/ar.1090170203.
2. Moran ET. Nutrition of the developing embryo and hatchling. Poult Sci. 2007;86:1043–9. https://doi.org/10.1093/ps/86.5.1043.
3. Bakhuis WL. Observations of hatching movements in the chick, Gallus domesticus. J Comp Physiol Psychol. 1974;87:997–1003. https://doi.org/10.1037/h0037206.
4. Gross GH. Innervation of the complexus ("Hatching") muscle of the chick. J Compar Neurol. 1985;232:180–9. https://doi.org/10.1002/cne.902320204.
5. De Oliveira JE, Uni Z, Ferket PR. Important metabolic pathways in poultry embryos prior to hatch. World's Poult Sci J. 2008;64:488–99. https://doi.org/10.1017/S0043933908000160.
6. Glaister M. Multiple sprint work: physiological responses, mechanisms of fatigue and the influence of aerobic fitness. Sports Med. 2005;35:757–77. https://doi.org/10.2165/00007256-200535090-00003.

7. Spriet LL. Anaerobic metabolism in human skeletal muscle during short-term, intense activity. Can J Physiol Pharmacol. 1992;70:157–65. https://doi.org/10.1139/y92-023.
8. Baker JS, McCormick MC, Robergs RA. Interaction among skeletal muscle metabolic energy systems during intense exercise. J Nutr Metab. 2010;2010:1–13. https://doi.org/10.1155/2010/905612.
9. Bessman SP, Carpenter CL. The creatine-creatine phosphate energy shuttle. Annu Rev Biochem. 1985;54:831–62. https://doi.org/10.1146/annurev.bi.54.070185.004151.
10. Rigdon RH, Ferguson TM, Trammel JL, Couch JR, German HL. Necrosis in the "pipping" muscle of the chick. Poult Sci. 1968;47:873–7. https://doi.org/10.3382/ps.0470873.
11. Marshall AF, Balloux F, Hemmings N, Brekke P. Systematic review of avian hatching failure and implications for conservation. Biol Rev. 2023;98:807–32. https://doi.org/10.1111/brv.12931.
12. Assersohn K, Marshall AF, Morland F, Brekke P, Hemmings N. Why do eggs fail? Causes of hatching failure in threatened populations and consequences for conservation. Anim Conserv. 2021;24:540–51. https://doi.org/10.1111/acv.12674.
13. Smith P, Daniel C. The chicken book. Boston, MA, USA: Little Brown & Co; 1975.
14. Sutherland DAT, Honaker CF, Dorshorst B, Andersson L, Brisbin IL, Siegel PB. Growth patterns for three generations of an intercross between red junglefowl and chickens selected for low body weight. J Anim Breed Genet. 2018;135:300–10. https://doi.org/10.1111/jbg.12336.
15. Fisher HI. The hatching muscle in North American Grebes. Condor. 1961;63:227–33. https://doi.org/10.2307/1365684.
16. Wolc A, White IMS, Hill WG, Olori VE. Inheritance of hatchability in broiler chickens and its relationship to egg quality traits. Poult Sci. 2010;89:2334–40. https://doi.org/10.3382/ps.2009-00614.
17. Fisher HI. The "hatching muscle" in the chick. Auk. 1958;75:391–9. https://doi.org/10.2307/4082098.
18. Smail JR. A possible role of the musculus complexus in pipping the chicken egg. Am Midl Nat. 1964;72:499. https://doi.org/10.2307/2423521.
19. Bock WJ, Hikida RS. An analysis of twitch and tonus fibers in the hatching muscle. Condor. 1968;70:211–22. https://doi.org/10.2307/1366693.
20. Ashmore CR, Addis PB, Doerr L, Stokes H. Development of muscle fibers in the complexus muscle of normal and dystrophic chicks. J Histochem Cytochem. 1973;21:266–78. https://doi.org/10.1177/21.3.266.
21. Christensen V, Donaldson W, Nestor K, McMurtry J. Effects of genetics and maternal dietary iodide supplementation on glycogen content of organs within embryonic turkeys. Poult Sci. 1999;78:890–8. https://doi.org/10.1093/ps/78.6.890.
22. Christensen VL, Grimes JL, Donaldson WE, Lerner S. Correlation of body weight with hatchling blood glucose concentration and its relationship to embryonic survival. Poult Sci. 2000;79:1817–22. https://doi.org/10.1093/ps/79.12.1817.
23. Christensen VL, Wineland MJ, Fasenko GM, Donaldson WE. Egg storage effects on plasma glucose and supply and demand tissue glycogen concentrations of broiler embryos. Poult Sci. 2001;80:1729–35. https://doi.org/10.1093/ps/80.12.1729.
24. Uni Z, Ferket RP. Methods for early nutrition and their potential. World's Poult Sci J. 2004;60:101–11. https://doi.org/10.1079/WPS20038.
25. Uni Z, Ferket PR, Tako E, Kedar O. In ovo feeding improves energy status of late-term chicken embryos. Poult Sci. 2005;84:764–70. https://doi.org/10.1093/ps/84.5.764.
26. Foye OT, Uni Z, Ferket PR. Effect of in ovo feeding egg white protein, β-hydroxy-β-methylbutyrate, and carbohydrates on glycogen status and neonatal growth of turkeys. Poult Sci. 2006;85:1185–92. https://doi.org/10.1093/ps/85.7.1185.
27. Yadgary L, Uni Z. Yolk sac carbohydrate levels and gene expression of key gluconeogenic and glycogenic enzymes during chick embryonic development. Poult Sci. 2012;91:444–53. https://doi.org/10.3382/ps.2011-01669.
28. Dayan J, Melkman-Zehavi T, Reicher N, Braun U, Inhuber V, Mabjeesh SJ, et al. Supply and demand of creatine and glycogen in broiler chicken embryos. Front Physiol. 2023;14:1079638. https://doi.org/10.3389/fphys.2023.1079638.
29. Wyss M, Kaddurah-Daouk R. Creatine and creatinine metabolism. Physiol Rev. 2000;80:1107–213. https://doi.org/10.1152/physrev.2000.80.3.1107.
30. Borchel A, Verleih M, Kühn C, Rebl A, Goldammer T. Evolutionary expression differences of creatine synthesis-related genes: Implications for skeletal muscle metabolism in fish. Sci Rep. 2019;9:5429. https://doi.org/10.1038/s41598-019-41907-6.
31. Ostojic SM. Creatine synthesis in the skeletal muscle: the times they are a-changin'. Am J Physiol-Endocrinol Metab. 2021;320:E390–1. https://doi.org/10.1152/ajpendo.00645.2020.
32. Freeman BM. The mobilization of hepatic glycogen in Gallus domesticus at the end of incubation. Comp Biochem Physiol. 1969;28:1169–76. https://doi.org/10.1016/0010-406X(69)90557-X.
33. Tazawa H, Visschedijk AHJ, Wittmann J, Piiper J. Gas exchange, blood gases and acid-base status in the chick before, during and after hatching. Respir Physiol. 1983;53:173–85. https://doi.org/10.1016/0034-5687(83)90065-8.
34. Sokale A, Peebles ED, Zhai W, Pendarvis K, Burgess S, Pechan T. Proteome profile of the pipping muscle in broiler embryos. Proteomics. 2011;11:4262–5. https://doi.org/10.1002/pmic.201000795.
35. Pulikanti R, Peebles ED, Keirs RW, Bennett LW, Keralapurath MM, Gerard PD. Pipping muscle and liver metabolic profile changes and relationships in broiler embryos on days 15 and 19 of incubation1,2. Poult Sci. 2010;89:860–5. https://doi.org/10.3382/ps.2009-00531.
36. García FJ, Pons A, Alemany M, Palou A. Tissue glycogen and lactate handling by the developing domestic fowl. Compar Biochem Physiol Part B: Compar Biochem. 1986;85:727–31. https://doi.org/10.1016/0305-0491(86)90168-9.
37. Høiby M, Aulie A, Bjonnes PO. Anaerobic metabolism in fowl embryos during normal incubation. Comp Biochem Physiol A Physiol. 1987;86:91–4. https://doi.org/10.1016/0300-9629(87)90282-9.
38. Liu Y, Song X, Liu W, Zhang T, Zuo J. Glucose deprivation induces mitochondrial dysfunction and oxidative stress in PC12 cell line. J Cell Mol Med. 2003;7:49–56. https://doi.org/10.1111/j.1582-4934.2003.tb00202.x.
39. Park H-H, Han M-H, Choi H, Lee YJ, Kim JM, Cheong JH, et al. Mitochondria damaged by oxygen glucose deprivation can be restored through activation of the pi3k/akt pathway and inhibition of calcium influx by amlodipine camsylate. Sci Rep. 2019;9:15717. https://doi.org/10.1038/s41598-019-52083-y.
40. Raut GK, Chakrabarti M, Pamarthy D, Bhadra MP. Glucose starvation-induced oxidative stress causes mitochondrial dysfunction and apoptosis via Prohibitin 1 upregulation in human breast cancer cells. Free Radical Biol Med. 2019;145:428–41. https://doi.org/10.1016/j.freeradbiomed.2019.09.020.
41. Martin M. Cutadapt removes adapter sequences from high-throughput sequencing reads. EMBnet J. 2011;17:10. https://doi.org/10.14806/ej.17.1.200.
42. Dobin A, Davis CA, Schlesinger F, Drenkow J, Zaleski C, Jha S, et al. STAR: ultrafast universal RNA-seq aligner. Bioinformatics. 2013;29:15–21. https://doi.org/10.1093/bioinformatics/bts635.
43. Anders S, Pyl PT, Huber W. HTSeq—a Python framework to work with high-throughput sequencing data. Bioinformatics. 2015;31:166–9. https://doi.org/10.1093/bioinformatics/btu638.
44. Love MI, Huber W, Anders S. Moderated estimation of fold change and dispersion for RNA-seq data with DESeq2. Genome Biol. 2014;15:550. https://doi.org/10.1186/s13059-014-0550-8.
45. Köster J, Rahmann S. Snakemake—a scalable bioinformatics workflow engine. Bioinformatics. 2012;28:2520–2. https://doi.org/10.1093/bioinformatics/bts480.
46. Ge SX, Jung D, Yao R. ShinyGO: a graphical gene-set enrichment tool for animals and plants. Bioinformatics. 2020;36:2628–9. https://doi.org/10.1093/bioinformatics/btz931.
47. Subramanian A, Tamayo P, Mootha VK, Mukherjee S, Ebert BL, Gillette MA, et al. Gene set enrichment analysis: a knowledge-based approach for interpreting genome-wide expression profiles. Proc Natl Acad Sci. 2005;102:15545–50. https://doi.org/10.1073/pnas.0506580102.

Publisher's Note